GeoScienceWorld
Lithosphere
Volume 2022, Article ID 3562869, 18 pages
https://doi.org/10.2113/2022/3562869

Lithosphere

Research Article

Petrology, Physical Properties, and Diagenetic Characteristics of Glutenite Reservoir: An Example from the Upper Urho Formation in Zhongguai Salient, Junggar Basin, China

Kang Zhao,[1] **Changming Zhang**,[1] **Liliang Huang**,[2] **Wenjun He**,[2] **Youlun Feng**,[2] **Qi Shuang**,[1] **and Jin Pan**[2]

[1]*School of Geosciences, Yangtze University, Wuhan 430100, China*
[2]*Research Institute of Exploration and Development, Xinjiang Oilfield Company, PetroChina, Karamay 834000, China*

Correspondence should be addressed to Changming Zhang; zcm@yangtzeu.edu.cn

Received 5 April 2022; Revised 20 September 2022; Accepted 29 September 2022; Published 25 October 2022

Academic Editor: Jingwei Huang

The Upper Urho Formation on the northwest margin of the Junggar Basin is a key formation for oil and gas exploration. Based on the core observation, combined with the analysis of cast thin section, scanning electron microscope, energy dispersive spectrum, X-ray diffraction, fluid inclusion, and porosity-permeability test, the petrological characteristics, physical properties, diagenesis types, and their effects on the physical properties of the glutenite reservoir of Upper Urho Formation were studied systematically. The results show that the lithology of reservoir of the Upper Urho Formation in Zhongguai Salient is mainly conglomerate with a small amount of sandstone. The permeability of conglomerate is generally higher than that of sandstone, and the physical properties of granule conglomerate and fine pebble conglomerate are relatively better. The reservoir experienced complicated diagenesis, mainly including compaction, cementation, and dissolution, also including filler shrink seam and metasomatism. At present, the reservoir of Upper Urho Formation in Zhongguai Salient is mainly at the middle diagenetic stage A period and partly at the middle diagenetic stage B period. The original porosity lost by compaction is the largest, which is the fundamental reason for low porosity and low permeability of reservoir. The influence of cementation on reservoir physical properties has two sides. On the one hand, the development of cementation is the main reason for low porosity and low permeability of reservoir. On the other hand, the early cementation resists compaction to a certain extent and provides a material basis for the later dissolution. The reservoir of Upper Urho Formation in Zhongguai Salient is deeply buried and has experienced strong compaction and cementation, and the reservoir properties are poor, but the secondary pore space formed by dissolution improves the reservoir properties to some extent. The study concluded that the dense glutenite reservoirs of the Upper Urho Formation can develop relatively high-quality reservoirs on a local scale, which is of guiding significance for the exploration of the Upper Urho Formation.

1. Introduction

Glutenites are mainly formed in near-source sedimentary systems such as alluvial fans, flood fans, and fan deltas with fast, unstable, and strong water flow [1–3]. The reservoirs formed by them are characterized by low rock maturity, wide particle size distribution, large physical variation, strong inhomogeneity, and rapid lateral changes, which in turn lead to limited discovery of glutenite oil fields, low reserve size, and slow progress of glutenite oil and gas research [3–5]. Since the 21st century, unconventional oil and gas have developed rapidly, showing huge resource potential and gradually becoming an important field of oil and gas exploration and development [6, 7]. As an important component of unconventional oil and gas, glutenite is rich in resources, with 74×10^8 t ~ 80×10^8 t geological resources

and 13×10^8 t ~ 14×10^8 t technical resources [8, 9], widely distributed in Junggar Basin, Bohai Bay Basin, and Songliao Basin [10–14].

The Junggar Basin is a typical large-scale superimposed petroliferous basin in western China [10, 11]. In recent years, with the discovery of the 1-billion-ton glutenite reservoir in the Mahu Sag, the overall study of the Permian and Triassic glutenite reservoirs in the Junggar Basin has been promoted [2, 4, 5, 10, 15]. Following the discovery of the glutenite reservoir of the Triassic Baikouquan Formation in the Mahu Sag, the glutenite reservoir of Upper Urho Formation (UUF) in the Permian has made another breakthrough in oil and gas, further confirming that the glutenite reservoir has huge exploration potential [4, 10, 16, 17]. The oil and gas exploration of the glutenite reservoirs in UUF of the Permian in the Zhongguai Salient (ZS) is a hot spot in recent years [18–21]. Scholars have focused on the macroscopic characteristics and depositional patterns of the glutenite reservoirs of UUF [18, 19, 21], but the research on the microscopic evolution, genetic mechanism, and controlling factors of the reservoirs is relatively weak.

Diagenesis is closely related to the exploration and development of petroliferous basins and is an important research field in sedimentary geology and petroleum geology [22–25]. As early as the 1970s, the research on the influence of diagenesis on sandstone and carbonate reservoirs began [26–28]. With the wide application of experimental testing techniques such as casting thin sections (CTS), scanning electron microscopy (SEM), energy dispersive spectrum (EDS), cathodoluminescence (CL), X-ray diffraction (XRD), fluid inclusion determination, and microbial diagenesis tracing, and the continuous innovation of research techniques and methods, diagenesis research has been developed rapidly [24, 25, 29]. Meanwhile, because of the huge resource potential of unconventional oil and gas reservoirs, scholars began to pay attention to the reservoir characteristics and diagenesis of conglomerate and shale. The conglomerate has large grain size, poor sorting, and strong heterogeneity. Scholars mainly use SEM, fluid inclusion, porosity and permeability testing, and other techniques to study the diagenesis and porosity evolution of conglomerate reservoir in combination with burial evolution history and oil and gas filling history [13, 18, 20, 30–33]. The particle size of mudstone is small, and the observation is difficult. In the last decade, the application of new techniques such as isothermal adsorption and SEM has enabled scholars to understand the nanoscale structure of mudstone, discover the presence of a large number of authigenic minerals, and deepen the understanding of organic and inorganic diagenesis in mudstone and its impact on reservoir quality [34–39].

In this study, the petrological characteristics, physical properties, and the type of diagenesis of the reservoir of UUF in the ZS are described, based on which the relationship between sediment grain size and physical properties is analyzed, the diagenetic sequence of UUF is analyzed, and finally, the influence of diagenesis on the physical properties of the reservoir is discussed. This study can provide reference for the prediction of high-quality glutenite reservoir and the evaluation of favorable zones of UUF of Permian in ZS.

2. Geological Setting

The Junggar Basin, located in northwestern China (Figure 1(a)), is an important petroliferous basin with an area of about 13.4×10^4 km^2 [40–45]. There are many mountains around the Junggar Basin, including Kelameili and Qingelidi mountains in the north-east, Bogda mountains to the south-east, Yilinheibiergen mountains in the south-west, and Hala'alate and Zhayier mountains to the north-west (Figure 1(b)) [20]. Based on gravity data and seismic data, the Junggar Basin can be divided into six primary tectonic units [20, 42], including three uplifts, two depressions, and onefold thrust belt (Figure 1(b)).

ZS is a secondary tectonic unit in the western uplift, located at the transition between the Ke-Wu Fault Zone and the Hongche Fault Zone, and at the lower plate of thrust fault zone (Figure 1(c)), and is a large inherited nose-like salient structure from Carboniferous to Jurassic [43, 44]. ZS has long been in the hydrocarbon transport pointing area of the three major hydrocarbon producing sags in Mahu, Penyijingxi, and Shawan and is one of the important hydrocarbon accumulation zones in the northwest margin of Junggar Basin, with an exploration area of about 2200 km^2 [18, 45]. The ZS is adjacent to the Dabasong salient to the east and transits to the Mahu Sag by slope in the northeast and to the Shawan Sag and the Penyijingxi Sag in the south in the form of monocline (Figure 1(c)) [45].

The widespread denudation of the upper part of Permian Jiamuhe Formation, Fengcheng Formation, Xiazijie Formation, and lower Urho Formation in ZS formed an unconformable contact relationship between Jiamuhe Formation and overlying UUF. The UUF and overlying Triassic Baikouquan Formation are also unconformable contact [4]. The UUF in ZS is a set of near-sourced gravelly sediments under the background of depression basin (Figure 1(d)). It is a large shallow-water regressive fan delta deposit in a gently sloping, wet environment setting [2, 10].

3. Samples and Methods

In this study, a total of 758.1 m of cores from 39 wells of UUF were observed and described, and the well location distribution is shown in Figure 1(c). CTS, SEM, EDS, XRD, fluid inclusions homogeneous temperature, and physical properties data were collected for these wells. All data used in this research originate from the Experimental and Testing Research Institute of the Xinjiang Oilfield, CNPC, which is a laboratory that meets the qualifications of Chinese industry certification standards.

CTS were prepared by vacuum impregnation with blue-dyed epoxy resin and stained with Alizarin Red S to facilitate recognition of carbonate cement. Through thin section observations, we can count the particle size, type, and content of clastic particles. At the same time, we can also determine the type and content of cement, as well as the type and percentage of pores. The types and phase of authigenic minerals can be used to determine diagenetic sequence.

SEM and EDS analyses were used to check the type of authigenic minerals and pore geometry. Observation was

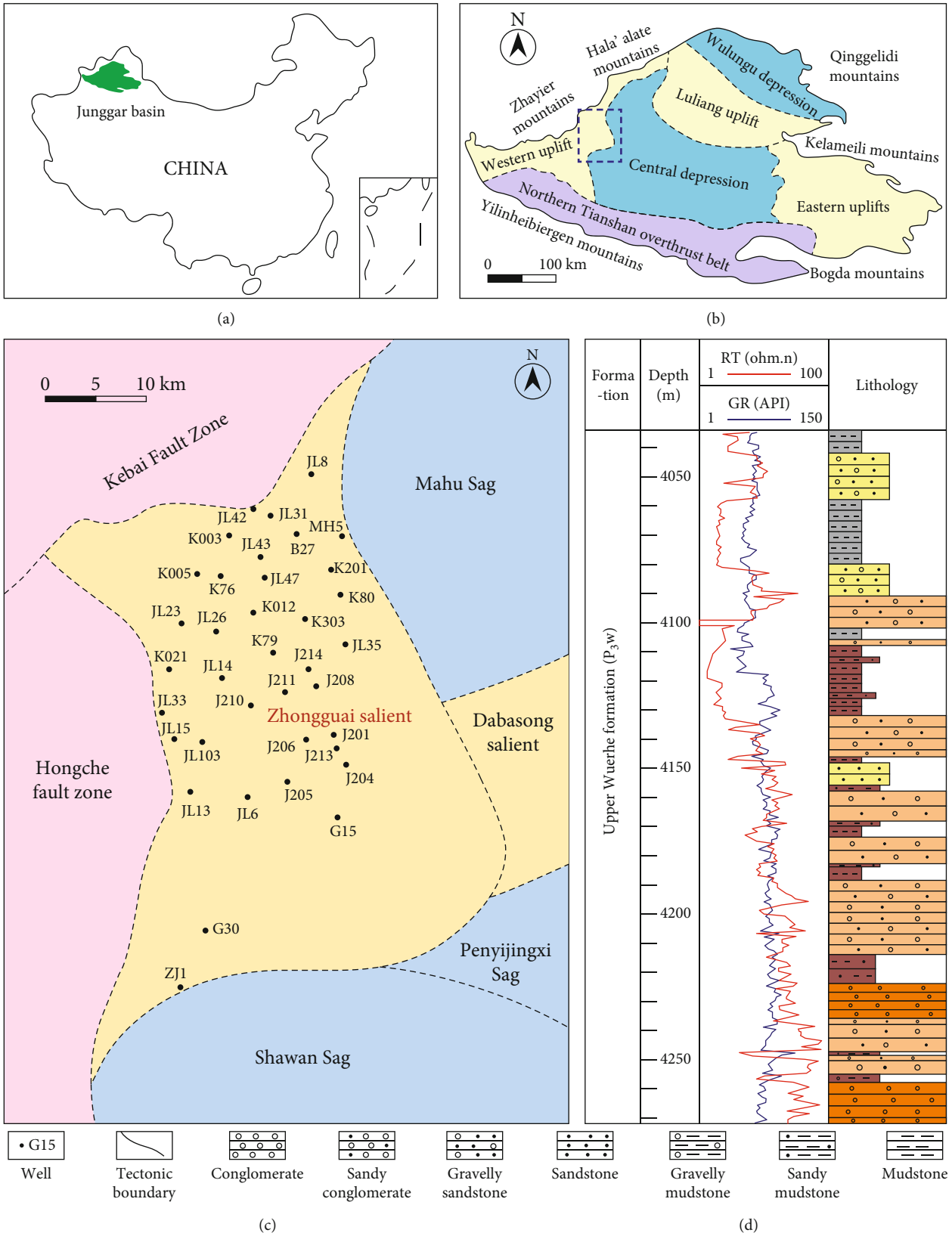

Figure 1: (a) Map of the Junggar Basin in China. (b) The division of tectonic units in the Junggar Basin and the location of Zhongguai Salient (ZS). (c) The division of subtectonic units around ZS. (d) Lithology of Upper Urho Formation (UUF) in well JL35 in ZS.

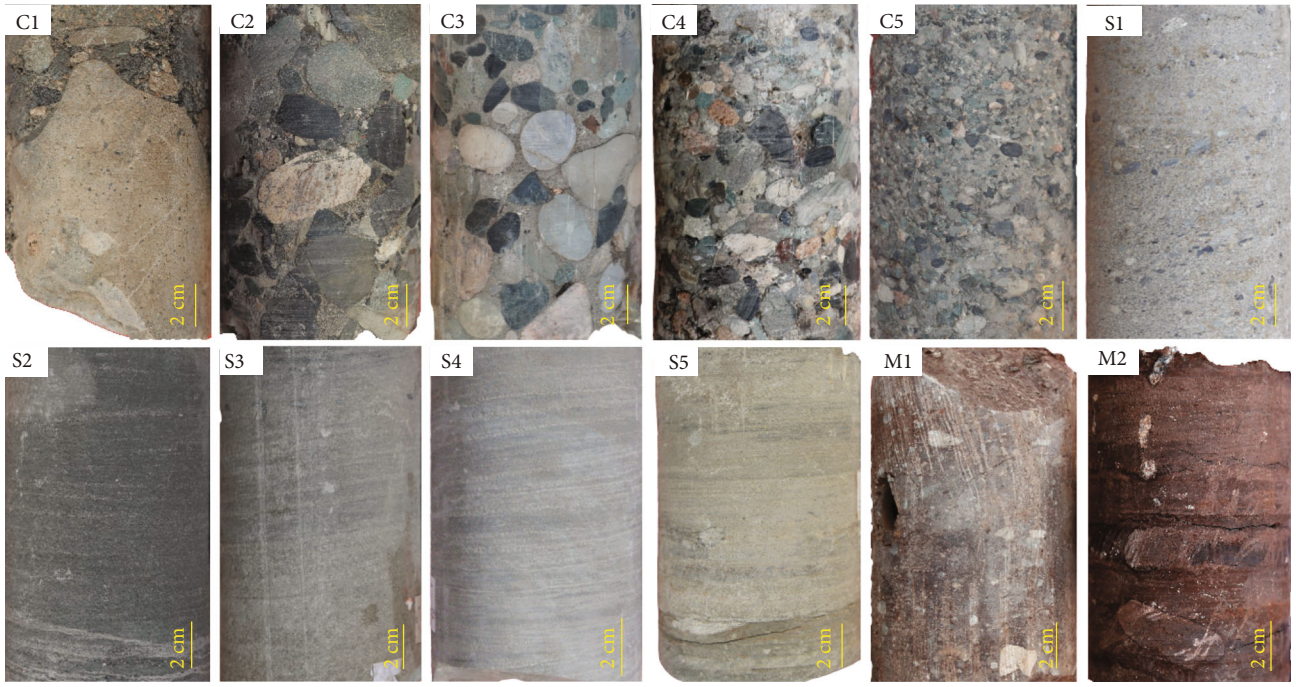

Figure 2: Photos of core samples of varied lithology of UUF in ZS. C1: boulder conglomerate, well JL47, 3302.81 m; C2: cobble conglomerate, well K304, 3658.7 m; C3: coarse pebble conglomerate, well K303, 3773.79 m; C4: fine pebble conglomerate, well J206, 4080.83 m; C5: granule conglomerate, well JW25, 3067.12 m; S1: very coarse sandstone, well J214, 3916.05 m; S2: coarse sandstone, well J205, 3840.18 m; S3: medium sandstone, well J213, 4152.18 m; S4: fine sandstone, well MH 11, 3461.41 m; S5: siltstone, well J208, 4044.26 m; M1: pebbly mudstone, well JL26, 3042.77 m; M2: mudstone, well MH015, 3638.99 m.

conducted using a FEI Quanta 250 FEG scanning electron microscope equipped with an energy dispersive spectroscope.

The relative abundances of the clay minerals were determined by XRD analysis, which can be used to determine the diagenetic sequence. Whole-rock mineral analysis used 200 mesh powder samples, and each mineral's mass percentage was calculated using an analysis software and referred to the K value of international standard samples. The relative mineral percentage was measured semiquantitatively.

Analysis of fluid inclusion types and occurrences was carried out using Leica DM2500P fluorescence microscope. The homogenization temperatures were determined using a Linkam THMS 600 microscope. The analytical error was small (±1°C) compared to the range of the results. The homogenization temperature can represent the temperature experienced in the diagenetic process and further be used to determine the diagenetic sequence.

The core porosity and permeability were analyzed using AP-608 Core Measurement system with a confining pressure of 6 MPa.

4. Results

4.1. Petrological Characteristics. The lithology of UUF is classified into three major categories: conglomerate, sandstone, and mudstone, denoted by C, S, and M, respectively. Conglomerates can be divided into five types: boulder conglomerate, cobble conglomerate, coarse pebble conglomerate, fine pebble conglomerate, and granule conglomerate, denoted by C1, C2, C3, C4, and C5, respectively. Sandstones can be divided into five types: very coarse sandstone, coarse sandstone, medium sandstone, fine sandstone, and siltstone, denoted by S1, S2, S3, S4, and S5, respectively. Mudstones are further divided into two types: pebbly mudstone and mudstone, denoted by M1 and M2, respectively (Figure 2).

The rocks of UUF have seven main colors: off-white, gray, gray-green, gray-brown, reddish-brown, gray-black, and black. The mudstone is mostly reddish-brown and gray-green, and the sandstone and conglomerate are mostly grayish-white, gray, gray-green, and gray-brown. The granular support of conglomerates of UUF can be divided into four types: grain-support, multiscale grain-support, matrix-grain-support, and matrix-support.

According to the statistics of the proportion of various lithology in the total core thickness (Figure 3), it can be found that UUF is mainly conglomerate, whose thickness accounts for about 70% of the thickness of the core section; sandstone is more developed, accounting for about 22%; and mudstone accounts for about 8%. The conglomerate is dominated by coarse pebble conglomerate, fine pebble conglomerate, and granule conglomerate, and its thickness accounts for about 85% of the total thickness of the conglomerate, while the sandstone is dominated by coarse sandstone, accounting for about 43% of the total thickness of the sandstone. In the observed 252.7 m sandstone section, the thickness of the gravelly sandstone and sandstone without gravel is approximately equal.

4.2. Physical Properties. Among the 1614 porosity data of glutenite samples from UUF, the maximum value is 25%,

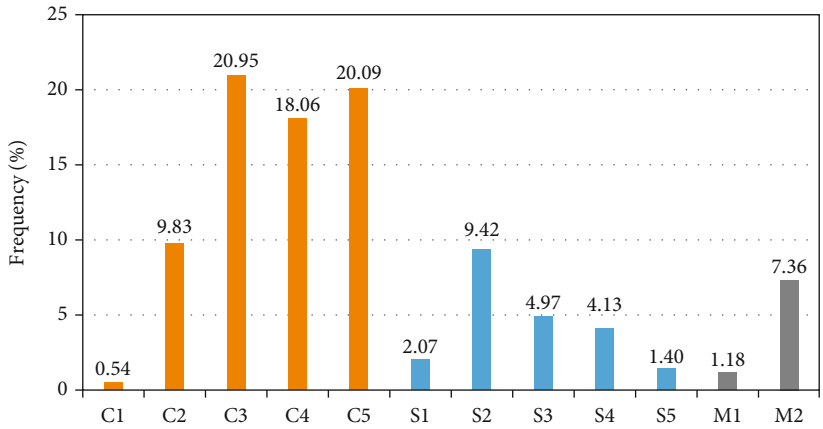

Figure 3: Frequency distribution of total thickness of various lithology in coring section.

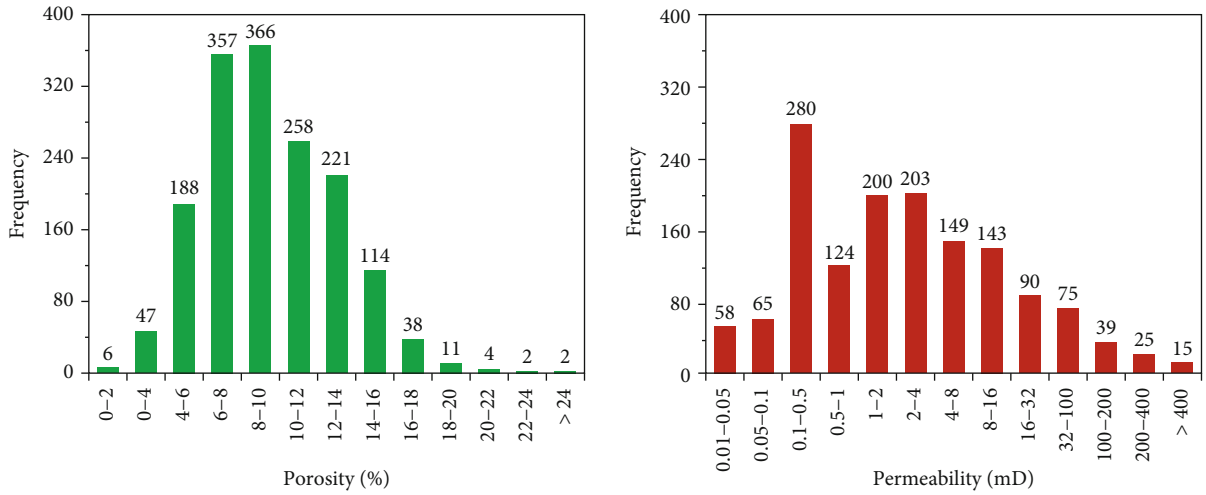

Figure 4: Histograms of porosity (a) and permeability (b) of UUF in ZS.

the minimum value is 0.5%, and the average value is 9.45%, and following the normal distribution (Figure 4(a)). There are 366 samples with porosity distribution between 8 and 10%, accounting for about 23%. There were 723 samples with porosity distribution between 6 and 10%, accounting for about 45%. There are 1390 samples with porosity distribution from 6 to 14%, accounting for about 86%.

The 1466 permeability data of glutenite samples from UUF are mainly concentrated between 0.1 and 4 mD, with 807 samples (55%) in this range (Figure 4(b)). There were 403 samples with permeability distribution between 1 and 4 mD, accounting for about 27%. There are 939 samples with permeability greater than 1 mD, accounting for about 64%. The maximum value of permeability for the sand and conglomerate samples of UUF is 958 mD, the minimum value is 0.01 mD, and the average value is 26.17 mD. The average value of permeability is obviously high, which is mainly due to the more developed fractures in the samples, especially in the conglomerate, resulting in large permeability in a few samples. These fractures may be artificially caused during sampling, which is difficult to avoid for conglomerate sampling; also, some fractures are natural, so these data were not discarded in this study. If the 90 samples with permeability greater than 100 mD are excluded, the average value of permeability at this time is 8.82 mD. If the 165 samples with permeability greater than 32 mD are excluded, the average value of permeability at this time is only 5.36 mD.

4.3. Diagenesis Types. Scanning electron microscopy and cast thin sections of the cores of UUF in ZS were analyzed, and it is concluded that the reservoir has experienced more complex diagenesis. The main diagenetic effects on the physical properties of the reservoir are compaction, cementation, and dissolution, while diagenetic shrinkage and accounting are also present in the target formation in ZS.

4.3.1. Compaction. The compaction of the reservoir in the target formation in ZS is strong, and the following phenomena can often be observed under the microscope: particle contact is mainly linear, but also concave-convex contact (Figure 5(a)) and suture line contact (Figure 5(b)); plastic particles are bent and deformed under compaction

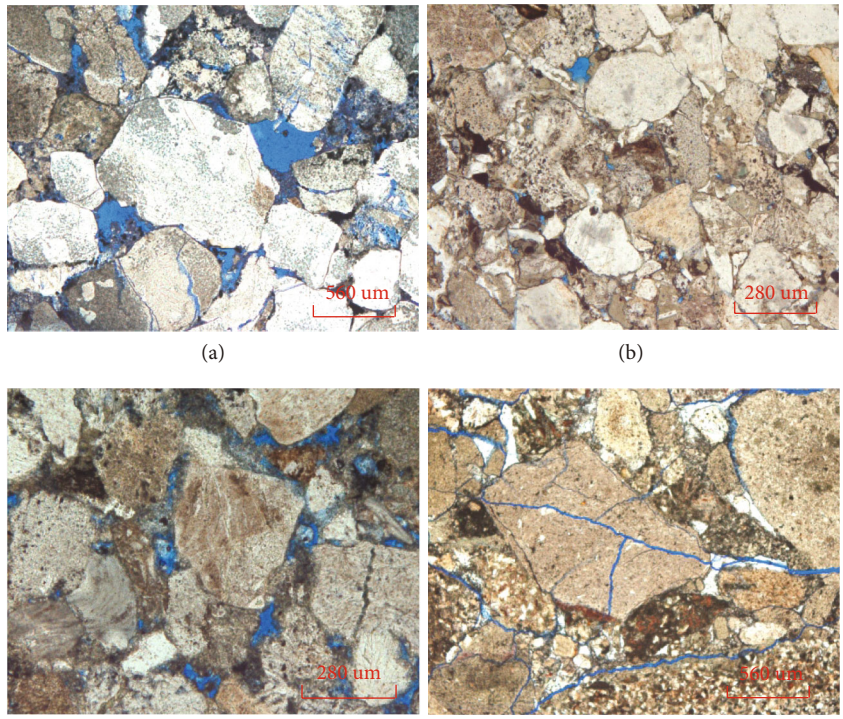

(a) (b) (c) (d)

FIGURE 5: Microscopic characteristics of compaction of glutenite reservoir of UUF in ZS. (a) Well J213, 4129.05 m, line-line contacts of particles, casting thin section, plane-polarized light; (b) well J201, 4122.25 m, concave/convex contacts and stylolite contacts of particles, casting thin section, plane-polarized light; (c) well 208, 4074.25 m, crushing of feldspar particles and deformation of ductile lithic fragment particles, casting thin section, plane-polarized light; (d) well 15, 3812.15 m, crushing of rigid particles, casting thin section, plane-polarized light.

(Figure 5(c)); and rigid clastic particles such as feldspar can be fractured by compaction (Figures 5(c) and 5(d)).

4.3.2. Cementation. Statistical analysis of cast thin sections and scanning electron microscopy showed that the types of cement of UUF in ZS are diverse, and common types of cement include carbonates (Figures 6(a)–6(d)), silica (Figures 6(e) and 6(f)), authigenic clay minerals (Figures 6(g)–6(k)), zeolites Figures 6(l) and 6(m)), and also ilmenite (Ilm) (Figure 6(d)), albite (Figure 6(n)), and pyrite (Figures 6(o) and 6(p)).

(1) Carbonate Cement. The carbonate cement of UUF in ZS is extremely developed, in which calcite is predominant. The crystals of carbonate cement formed in early diagenesis are small. The calcite crystals formed in the middle and late stages of diagenesis are larger and often fill the intergranular pores in a stellate and mosaic manner (Figure 6(a)), with a dark red color under the cast thin section (Figure 6(b)); dolomite (Figure 6(c)) and a small amount of apatite (Ap) are also developed (Figure 6(d)). Both calcite and dolomite contain K, Na, Fe, Si, etc., with Ca : Mg (ratio of atoms) = 1 : 1-2.7 : 1 in dolomite.

(2) Siliceous Cement. Siliceous cement of UUF in ZS is mainly in the form of small quartz crystals growing on the surface of intergranular pores (Figures 6(e) and 6(f)). It is generally believed that the siliceous cement $Si0_2$ originated from pressure solubility or dissolution of feldspar or interconversion of clay minerals [46, 47]. In the core thin section of UUF in ZS, pressure dissolution was observed only locally, while authigenic quartz and quartz secondary enlargement were common in SEM, so it is believed that SiO_2 in the target reservoir in ZS mainly originates from kaolinization of feldspar in acidic media environment.

(3) Authigenic Clay Minerals. X-ray diffraction analysis shows that clay minerals are commonly developed in reservoir of UUF in ZS (Table 1), and common clay minerals include chlorite (Figure 6(g)), illite (Figure 6(h)), kaolinite (Figure 6(i)), and illite/smectite mixed layer (Figure 6(j)), while monzonite cementation (Figure 6(k)) is rare. Chlorite is mostly blade-like growing perpendicular to the surface of the clastic particles (Figure 6(g)). Under the acidic medium, kaolinite was formed by the dissolution of feldspar particles and friable lithic fragments of the glutenite reservoir in ZS, and under the scanning electron microscope, kaolinite mostly appeared as worm-like or page-like aggregates filled in the intergranular pores (Figure 6(i)).

(4) Zeolite Cement. The ZS is close to the western source, and the reservoir of UUF has a high content of tuff and other volcanic lithic fragments, and the dissolution of volcanic material under the action of pore fluids during the burial diagenesis provides the material basis for the formation of zeolite-like cement [48–50]. For the reservoirs of UUF in

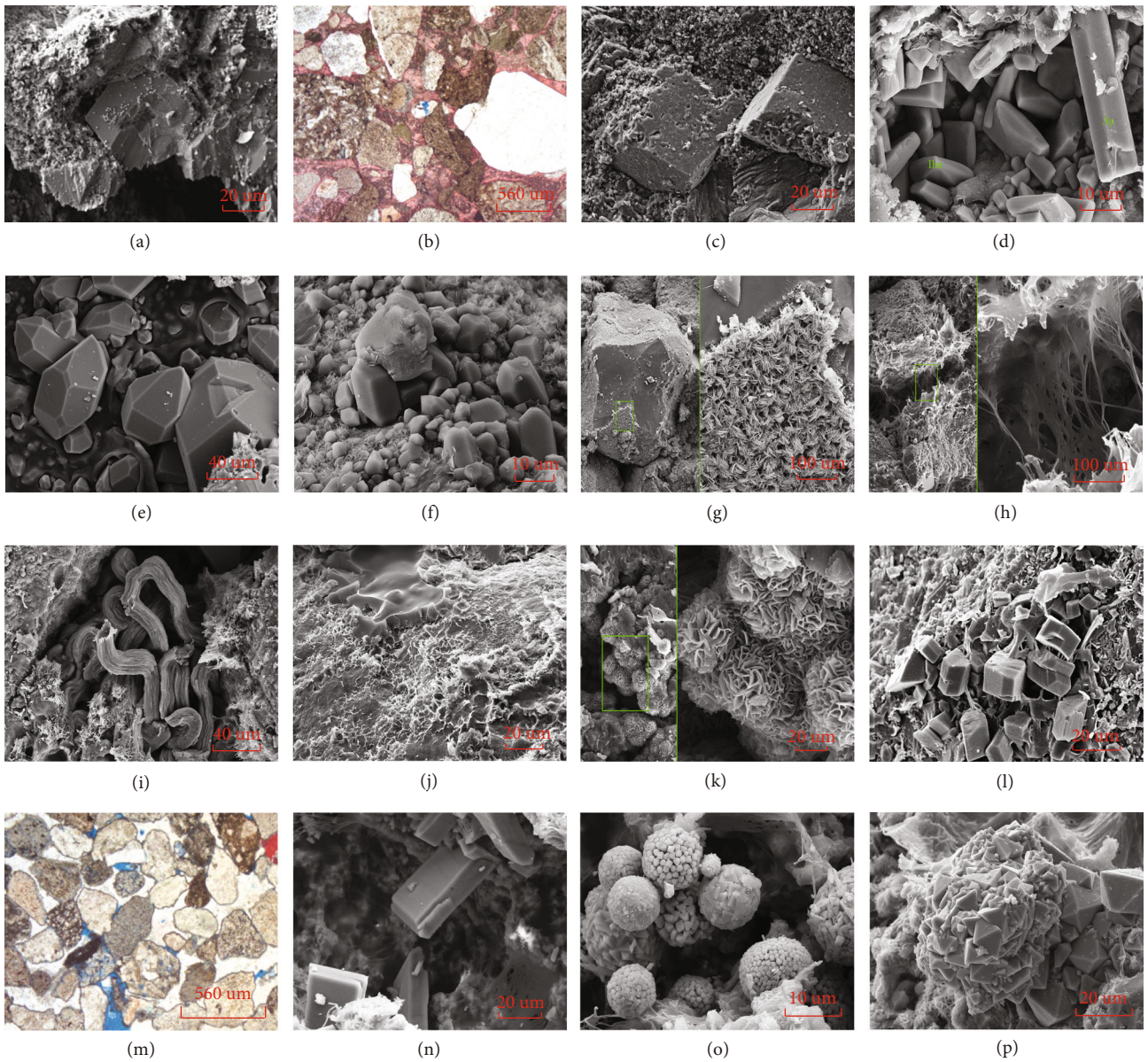

Figure 6: Types and characteristics of cement of UUF in ZS. (a) Well K303, 3676.5 m, calcite imbedded cement among particles, SEM; (b) well B27, 3360.8 m, calcite cement filled between particles, casting thin section; (c) well JL42, 2886.13 m, dolomite cement imbedded among particles, SEM; (d) well JL42, 2918.9 m, columnar apatite crystals (Ap) and tabular ilmenite crystals (Ilm) filled between particles, SEM; (e) well K303, 3677.1 m, authigenic quartz crystallites grow on the surface of particles, SEM; (f) well K303, 3677.1 m, authigenic quartz crystals grow on the surface of particles, SEM; (g) well K101, 3612.8 m, petal-shaped chlorite cement grow on the surface of particles, SEM; (h) well JL42,2850.68 m, filamentous illite cement in pores between particles, SEM; (i) well JL42, 2894.03 m, vermicular kaolinite cement in pores between particles, SEM; (j) well K304, 3672 m, irregular shape of illite/smectite mixed layer cement on the surface of particles, SEM; (k) well JL42, 2847.84 m, leaf-shaped smectite cement mass in pores between particles, SEM; (l) well 303, 3740.9 m, laumontite cement in pores between particles, SEM; (m) well J205, 3814.3 m, laumontite cement in pores between particles, casting thin section, plane-polarized light; (n) well JL42, 2914.68 m, tabular albite crystals in pores between particles, SEM; (o) well JL42, 2914.68 m, spheroidal pyrite aggregation in pores between particles, SEM; (p) well 42, 2879.28 m, aggregate of octahedral pyrite on the surface of particles, SEM.

ZS, zeolite-like minerals occur as cement and fracture fillings, which are commonly found in intergranular pores and intragranular solution pores (Figures 6(l) and 6(m)).

4.3.3. Dissolution. There are many components in which dissolution occurs, mainly including clastic particles and colluvium.

(1) Clastic Particles. The glutenite of UUF in ZS is rich in feldspar particles and volcanic rock clastic particles, so they are susceptible to dissolution under suitable conditions to form various clay minerals. The feldspar grains are mostly dissolved along the detrital suture, which can be seen as patchy dissolution pores (Figure 7(a)) or honeycomb dissolution pores (Figure 7(b)) under scanning electron microscopy, and

Table 1: X-ray diffraction analysis of clay minerals of reservoir of UUF in ZS.

Well name	Number of samples	Relative average content of clay minerals					
		Smectite	Illite/smectite mixed layer	Illite	Kaolinite	Chlorite	Chlorite/smectite mixed layer
J204	3	0	17.70	5.70	0	76.60	0
J206	15	0	60.00	6.50	12.00	21.50	0
J208	28	0	49.00	5.50	8.60	36.90	0
J210	4	0	72.50	2.75	0	24.75	0
J211	4	0	23.50	7.25	14.00	55.25	0
J214	2	0	32.50	4.50	0	63.00	0
JL33	1	0	36.00	14.00	41.00	9.00	0
JL42	14	39.40	41.60	3.70	7.00	8.30	0
JL15	12	0	64.00	30.20	0.13	5.67	0
ZJ6	13	0	8.30	5.40	0	56.50	29.80

the feldspar is dissolved to form speckled intragrain dissolution pores in rock thin section (Figure 7(c)). When dissolution occurs at the edges of rock chip particles, irregularly enlarged intergranular pores are often formed, and when dissolution occurs locally, long, speckled intragranular pores are easily formed (Figures 7(d) and 7(e)).

(2) Cement. Carbonate cement, especially calcite cement, is very well developed in glutenite reservoirs of UUF in ZS, and during diagenesis, pore fluids undergo dissolution of carbonate cement to form pores under suitable pH and Pco2 values [18, 46]. Calcite cement mostly forms intergranular pores under dissolution (Figure 7(f)), and even the crystals are completely dissolved (Figure 7(g)). Turbidite colluvium is widely distributed in the sand and gravels of UUF in ZS, and dissolution of laumontite mostly forms pores in crystals (Figure 7(h)), and widespread dissolution of laumontite is also common (Figure 7(i)).

(3) Matrix. The glutenite reservoirs of UUF in ZS have a high content of heterogeneous groups, and under suitable conditions, the gap-filling dissolution pores formed by dissolution of heterogeneous groups can also improve the reservoir physical properties. The statistical analysis in [43] concluded that the heterogeneous base dissolution pores are the more developed dissolution pores in the Permian reservoirs in ZS.

4.3.4. Other Types of Diagenesis. Interstitial material shrinkage and mineral metasomatism can also be observed in the reservoirs of UUF in ZS. Interstitial material shrinkage is an effect of dewatering and shrinking of mud-filled matrix during diagenetic compaction of large-grained, well-rounded conglomerates [51, 52]. Interstitial material shrinkage often forms seams distributed along the edges of the gravels (Figures 8(a) and 8(b)). Mineral metasomatism is the process by which minerals are dissolved and simultaneously replaced by other minerals precipitated in the pore fluid and can reveal the sequence of mineral formation [46]. The common laumontite cement of UUF in ZS replaces the calcite cement formed in the early stage (Figures 8(c) and 8(d)).

5. Discussion

5.1. The Relationship between Rock Grain Size and Physical Properties. A total of 1286 samples with both porosity and permeability were measured in this study, including 824 conglomerate samples and 462 sandstone samples. The relationship between porosity and permeability was analyzed in two lithologies, conglomerate and sandstone (Figure 9). The cross plot shows that there exists a better differentiation between conglomerate and sandstone, which shows that the permeability of conglomerate is generally larger than that of sandstone. The main distribution interval of permeability of conglomerate is 0.7-20 mD, and that of sandstone is 0.2-3 mD. The coefficient of determination (R^2) of the fitting function of porosity and permeability is 0.0746 for the conglomerate and 0.2226 for the sandstone, indicating that the correlation between porosity and permeability of the sandstone reservoir is significantly better than that of the conglomerate, and it is assumed that the fractures are more developed in the conglomerate.

In order to clarify the physical property differences between conglomerates of different grain sizes of UUF in ZS, cross plots of porosity and permeability were made for various types of conglomerates, and their trend lines were fitted (Figure 10). Due to the grain size of the boulder conglomerate exceeds the core diameter, it is difficult to obtain their physical property data, and the boulder conglomerates are not considered in the data analysis.

The number of coarse conglomerate samples is 62, and the coefficient of determination of the fitting function is 0.0111 (Figure 10(a)); the number of large and medium conglomerate samples is 190, and the coefficient of determination of the fitting function is 0.1353 (Figure 10(b)); the number of small and medium conglomerate samples is 231, and the coefficient of determination of the fitting function is 0.1241 (Figure 10(c)); the number of fine conglomerate samples is 341, and the coefficient of determination of the fitting function is 0.0518 (Figure 10(d)). The coefficient of determination is larger for the coarse pebble conglomerate and the fine pebble conglomerate, and the cobble conglomerate has the smallest coefficient of determination, reflecting that the correlation between porosity and permeability is

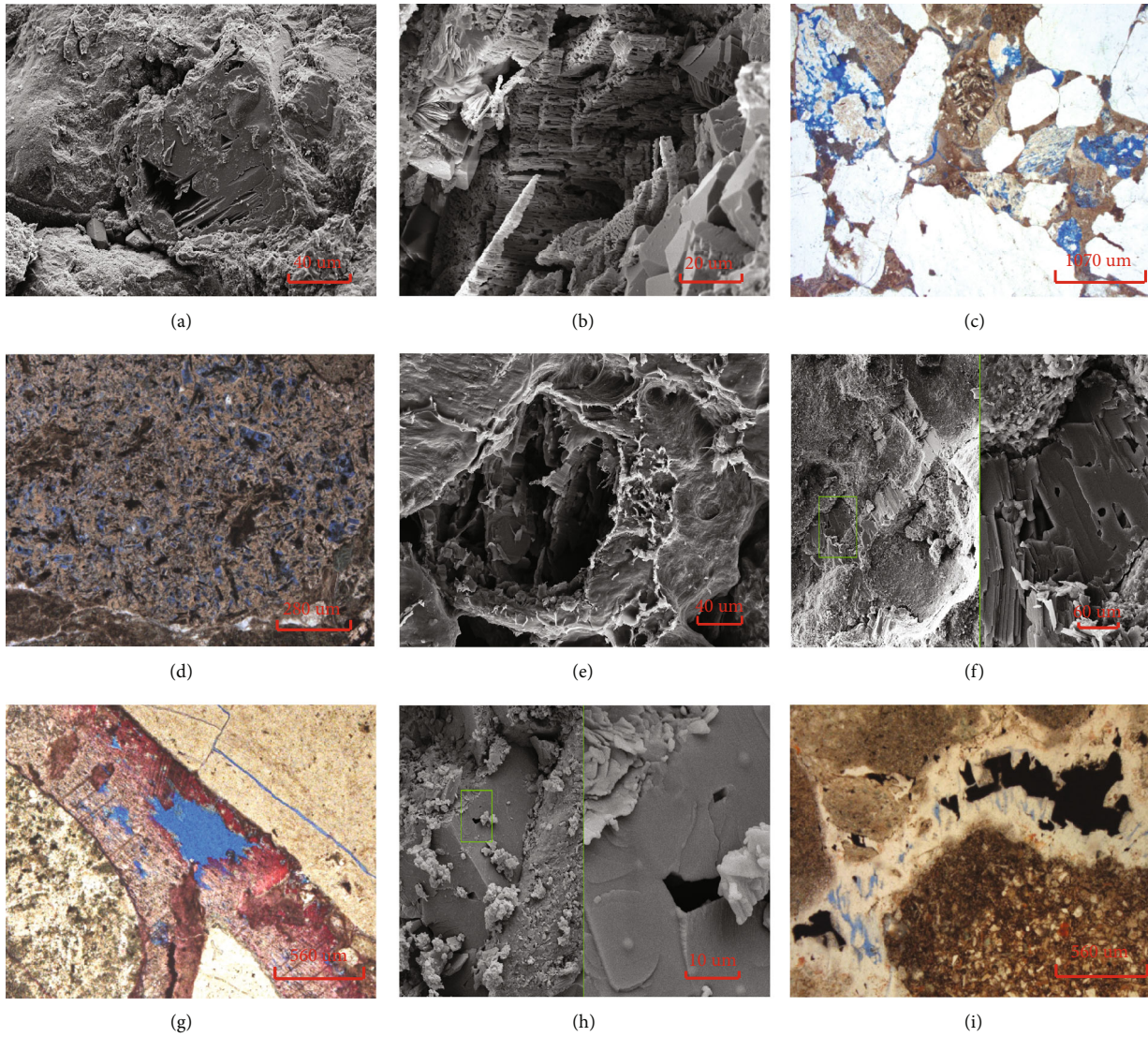

Figure 7: Microscopic characteristics of dissolution of glutenite reservoir of UUF in ZS. (a) Well K79, 3477.3 m, intragranular dissolution pores of feldspar, SEM; (b) well ZJ6, 4847.69 m, dissolution pores of feldspar along cleavage crack, SEM; (c) well B27, 3216.46 m, intragranular dissolution pores of feldspar, casting thin section, plane-polarized light; (d) well 42, 2825.36 m, intergranular dissolution pores of volcanic lithic fragment, casting thin section, plane-polarized light; (e) well JL42, 2865.91 m, intergranular dissolution pores of volcanic lithic fragment, SEM; (f) well ZJ6, 4850.68 m, dissolution pores of calcite cement, SEM; (g) well JL31, 3046.41 m, dissolution pores of calcite cement, casting thin section, plane-polarized light; (h) dissolution pores of laumontite cement, SEM; (i) dissolution pores of laumontite cement, casting thin section, plane-polarized light.

more obvious for the coarse pebble conglomerate and the fine pebble conglomerate, indicating that these two lithologies are the better reservoirs in the conglomerate. The highest ratio of the number of samples with porosity greater than 12% is the granule conglomerate, followed by the fine pebble conglomerate, a phenomenon thought to be related to sediment sorting. Based on the results of detailed observations and descriptions of the cores, it is found that the granule conglomerate has the relatively best sorting, mainly good-moderate; the fine pebble conglomerate has mainly moderate sorting, while the coarse pebble conglomerate and cobble conglomerate have mainly moderate-poor sorting. The better the sorting of the sediments, the more original intergranular pores, and the more remaining intergranular pores after diagenesis, the greater the porosity.

5.2. Stages of Diagenetic Evolution. The glutenite reservoir of UUF in ZS is deeply buried, generally at a depth of 2500-4500 m. The glutenite is well cemented and subject to strong compaction. The clastic grains are mainly in line contact, with some grains showing concave-convex contact and even rupture (Figure 5). The physical properties of the reservoir are generally poor, the original pore space has been lost in large quantities, and the pore space type is mainly secondary pore space such as intragrain solution pore and intergrain solution pore, with a small amount of microfractures and

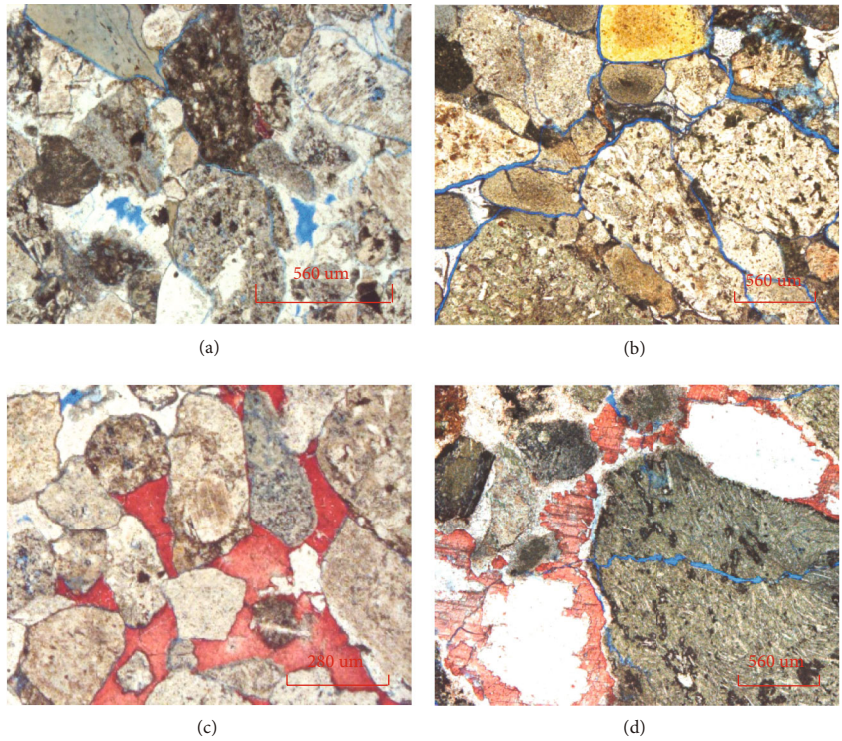

Figure 8: Microscopic characteristics of interstitial material shrinkage and mineral metasomatism of glutenite reservoir of UUF in ZS. (a) Well J201, 4115.44 m, interstitial material shrinkage, casting thin section, plane-polarized light; (b) well J201, 4115.44 m, interstitial material shrinkage, casting thin section, plane-polarized light; (c) well J205, 3814.3 m, laumontite cement metasomatic calcite cement, casting thin section, plane-polarized light; (d) well ZJ6, 4947.22 m, laumontite cement metasomatic calcite cement, casting thin section, plane-polarized light.

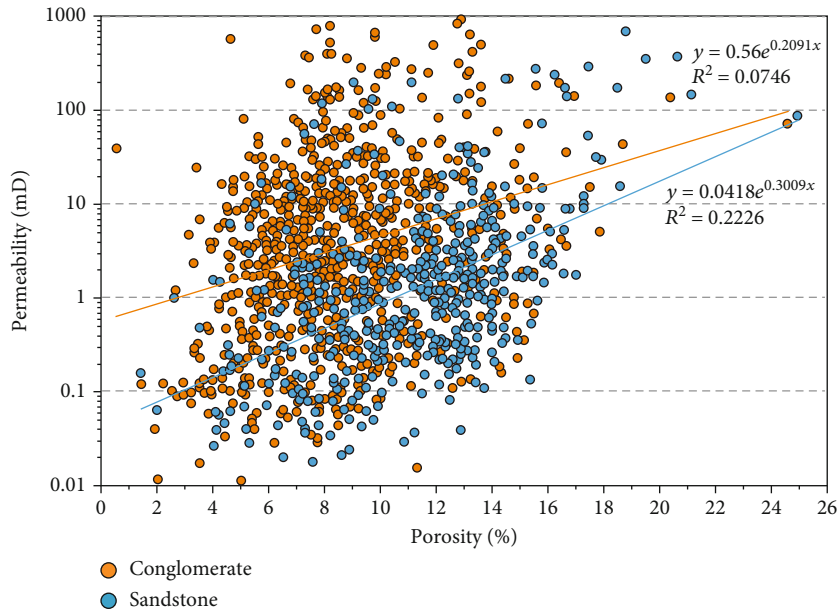

Figure 9: Cross plot of permeability and porosity of conglomerate and sandstone of UUF in ZS.

intercrystal micropores developed (Figures 4 and 7). Authigenic minerals such as laumontite, illite, and chlorite are common in the reservoir, kaolinite and dolomite can be seen, and monazite has basically disappeared (Table 1). The dissolution of calcite cement and laumontite cement is commonly developed (Figures 7 and 8). The rock-forming environment of glutenite reservoir of UUF in ZS is a coexistence of faintly acidity and alkalescence [53].

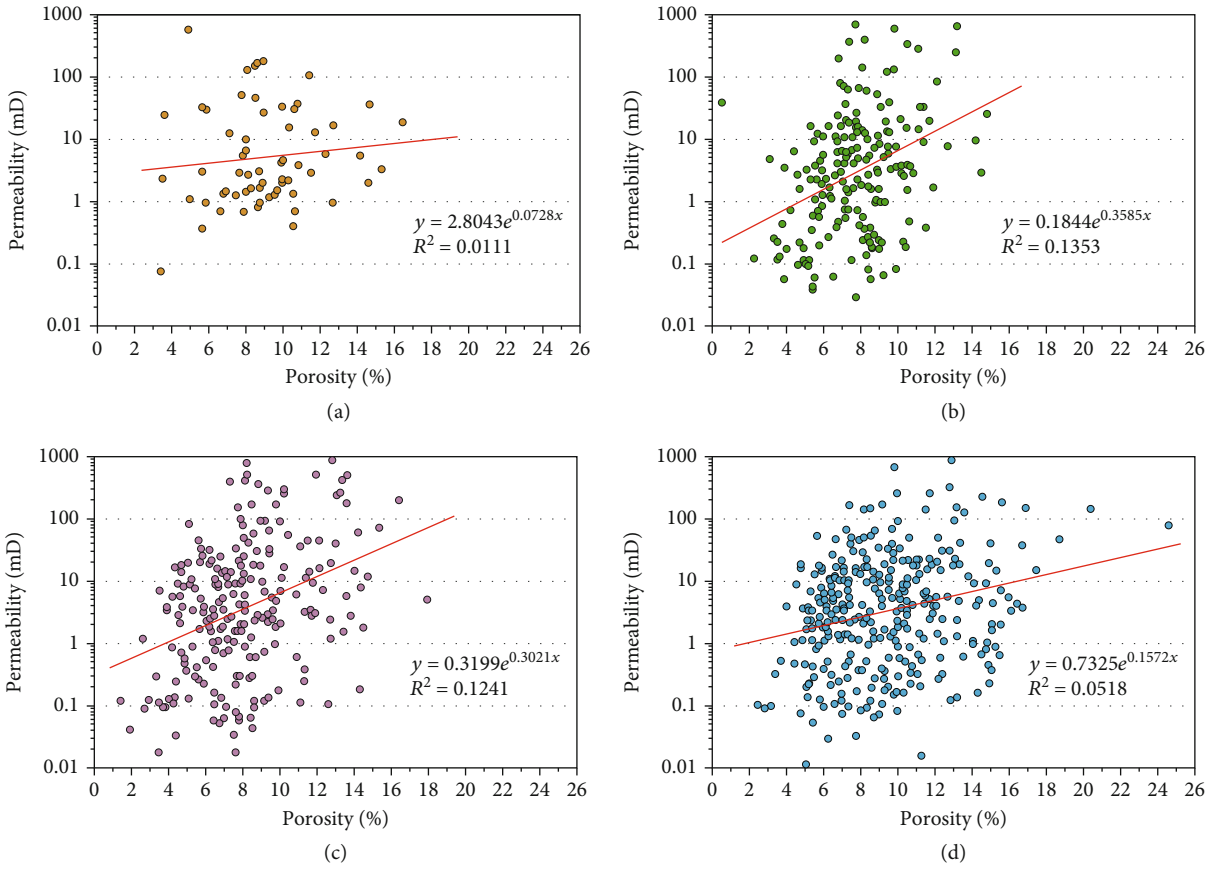

Figure 10: Cross plots of permeability and porosity of cobble conglomerate (a), coarse pebble conglomerate (b), fine pebble conglomerate (c), and granule conglomerate (d) of UUF in ZS.

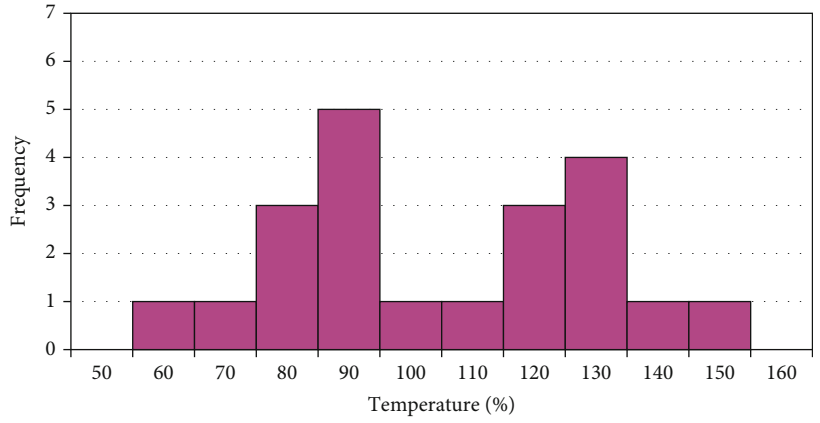

Figure 11: The homogenization temperature distribution of fluid inclusions of UUF in ZS.

Fluid inclusion homogenization temperatures were determined in 21 reservoir samples from UUF (Figure 11). Fluid inclusion homogenization temperatures of 60°-150° were occurred, mainly distributed in 80°-130°, showing a continuous double-peaked pattern. Salt water inclusions and hydrocarbon inclusions exist in UUF, mainly in the secondary enlarged part of quartz grains and within microfractures (Figure 12). A small number of inclusions exist in feldspar grains, but they are not suitable for temperature measurement. The particle size of inclusions in quartz grains is 0.1 μm-10.4 μm.

The diagenetic stages of glutenite reservoirs of UUF in ZS were divided based on parameters such as contact characteristics of grains, authigenic mineral assemblages, pore morphology characteristics and dissolution characteristics, and fluid inclusion homogeneous temperature data with

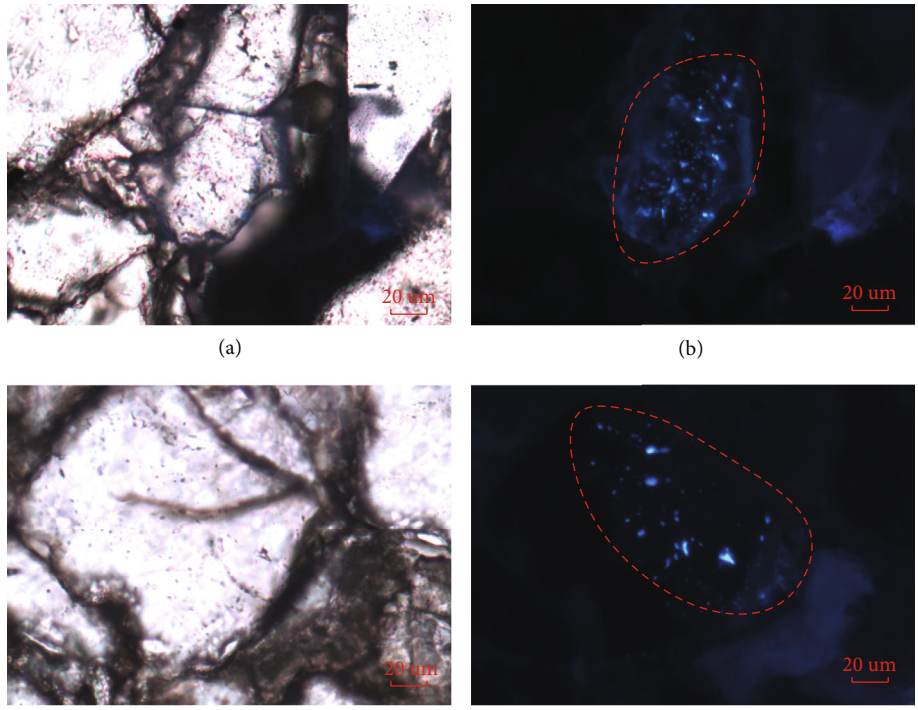

Figure 12: Fluid inclusion characteristics of UUF in ZS. (a) Well J201, 4105.38 m, fluid inclusion, casting thin section, plane-polarized light; (b) well J201, 4105.38 m, mainly shows hydrocarbon inclusions, casting thin section, fluorescent photograph; (c) well J205, 3814.3 m, fluid inclusion, casting thin section, plane-polarized light; (d) well ZJ6, 4947.22 m, mainly shows hydrocarbon inclusions, casting thin section, fluorescent photograph.

reference to the diagenetic stage division criteria of [54]. It is concluded that the glutenite reservoir of UUF in ZS is mainly in the middle diagenetic stage A period, and some have entered the middle diagenetic stage B period (Figure 13).

By analyzing the type of diagenesis, the genesis and generation time of authigenic clay minerals, and the homogeneous temperature of fluid inclusions, the sequence of diagenesis in ZS can be determined as follows: mechanical compaction-early clay film formation-early mud crystal calcite cementation-quartz secondary increase-massive zeolite type cementation-acidic fluid activity (hydrocarbon charging)-feldspar particle dissolution-authigenic kaolinite formation-calcite cementation dissolution-zeolite type cementation dissolution-acidic fluid activity (hydrocarbon charging)-late iron calcite and iron dolomite filling.

5.3. Effect of Diagenetic on Reservoir Physical Properties

5.3.1. Effect of Compaction on Reservoir Physical Properties. The UUF of Permian in ZS contains more volcanic lithic fragment and a certain amount of argillaceous matrix. The volcanic lithic fragment is prone to bending and deformation under the compaction stress and occupy the intergranular pores, so that the volume of original pores is rapidly reduced. At the same time, the argillaceous matrix inhibits the development of carbonates and other cement to a certain extent, resulting in the lack of support of carbonates and other cement as a supporting framework in the sediments at the early stage of diagenesis, which makes the compaction more likely to destroy the original pore space in the sediments and cause the original porosity to decrease [51, 55, 56]. The buried depth of the reservoir of UUF in ZS is between 2500 m and 4500 m, and the compaction has significantly damaged the pore space of the reservoir, and the contact mode of the clastic particles is mainly line contact, and some of them appear concave-convex contact or even stylolite contact (Figure 5(b)), indicating a strong degree of compaction.

In this study, the relationship between compaction, cementation, and intergranular original porosity loss was made through statistical analysis of cementation content and porosity data of the glutenite reservoir of UUF in ZS, which can quantify the loss of original intergranular pore volume in the reservoir under compaction. The results showed that the compaction caused the maximum loss of original porosity of the glutenite reservoir of UUF up to 85%, and the main distribution range was 35%-75% (Figure 14), indicating that the strong mechanical compaction was the most important factor causing the loss of original porosity in the reservoir of UUF in ZS.

5.3.2. Effect of Cementation on Reservoir Physical Properties. The cement in the reservoir of UUF in ZS includes authigenic clay mineral cement, carbonate cement, zeolite cement, siliceous cement, and so on. The loss of original porosity caused by these cementations can be up to 70%, and the loss of original porosity is mainly 5%-40% (Figure 14), indicating that

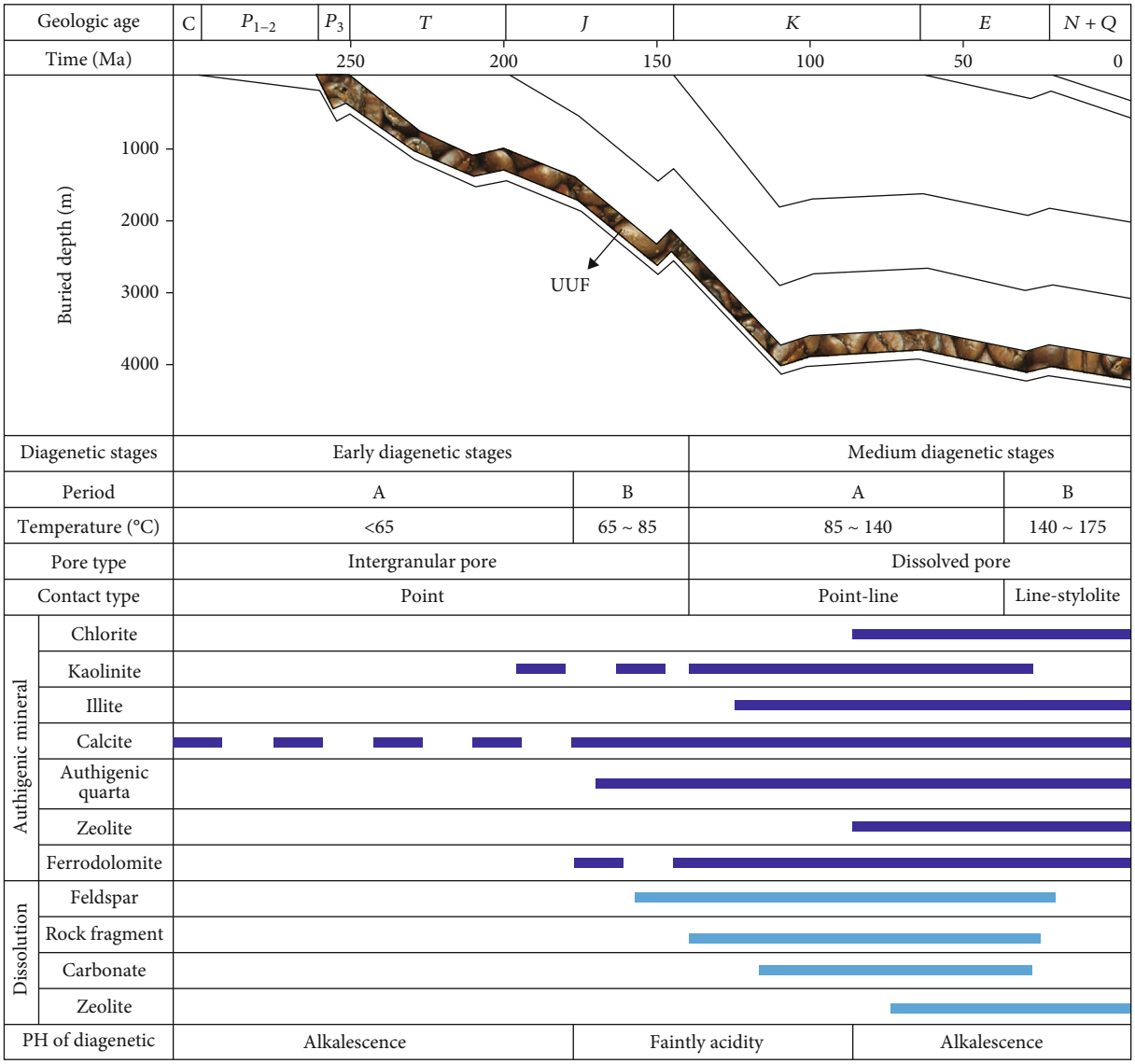

Figure 13: Diagenetic sequence of UUF in ZS.

the cementation of the reservoir of UUF in ZS is more developed and is the main factor for the loss of original porosity of the reservoir, but its damage to the reservoir pore space is smaller than that of compaction.

Different clay minerals have different effects on reservoir physical properties. Analysis of the relationship between the relative content of clay minerals (the ratio of clay mineral content to cement content) and porosity showed that chlorite content, kaolinite content, and porosity were significantly positively correlated (Figures 15(a) and 15(b)), while illite/smectite mixed layer content, illite content, and porosity were significantly negatively correlated (Figures 15(c) and 15(d)). Chlorite content was formed mainly during the early diagenetic period [46, 57]. Chlorite cemented along the edge of intergranular pore space resists the destruction of original pore space by compaction to a certain extent, and chlorite films growing around the edge of the grains hinder the further reaction between grains and fluids in pores, effectively inhibiting the increase of secondary quartz and facilitating the preservation of original intergranular pore space. Kaolinite is mostly formed in acidic fluid environment, and previous studies [51, 58] concluded that kaolinite is usually formed by the dissolution of aluminosilicate minerals such as feldspar and clay matrix and is an indicator mineral for secondary pore development, so the higher the content of kaolinite the better the reservoir physical properties in general. Illite/smectite mixed layer is an intermediate product of transformation from smectite to illite, mostly in the form of flakes and fibers, and its massive development can block the pores and throats and reduce the physical properties of the reservoir. With the increase of formation pressure and temperature, the content of potassium ions in the formation gradually increases, and the illite/smectite mixed layer will be transformed into illite, which extends farther in the pore space than other authigenic clay minerals and often fills the small pores and throats in the form of needles and hairs, which seriously destroys the permeability and effective porosity of the reservoir.

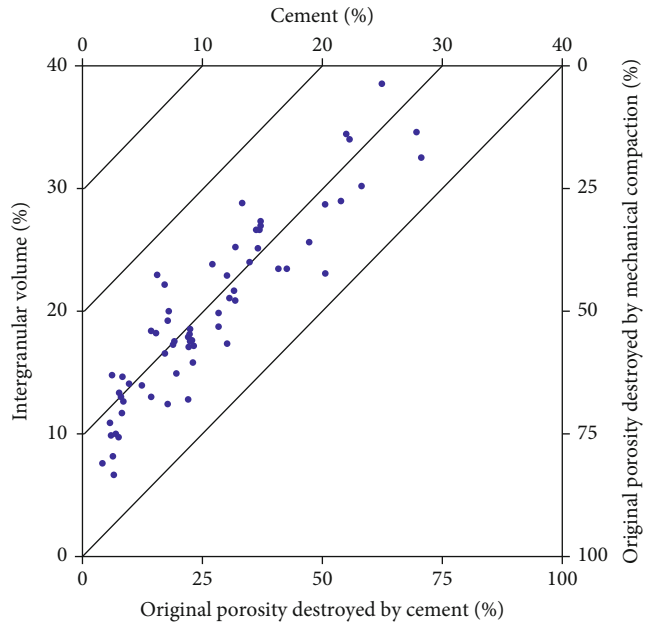

Figure 14: Plot of original porosity reduction between cementation and compaction of UUF in the ZS.

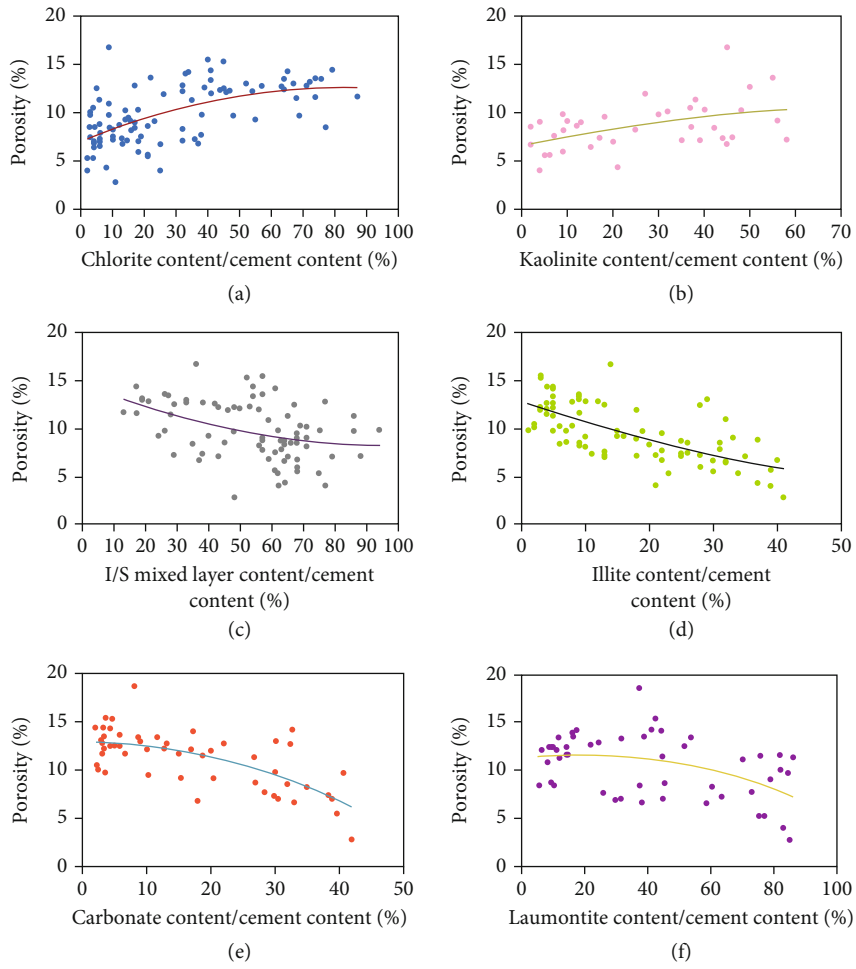

Figure 15: Relationships between the relative content of different types of cement with porosity of UUF in ZS: (a) chlorite cement; (b) kaolinite cement; (c) I/S mixed layer cement; (d) illite cement; (e) carbonate cement; (f) laumontite cement.

Carbonate cement is commonly developed in the reservoir of ZS in ZS, and their contents show an obvious negative correlation with porosity (Figure 15(e)). Carbonate cement can be formed in all periods of diagenesis, and the crystals of carbonate cement formed in early diagenesis are small and can be used as skeletal particles to reduce the damage of reservoir properties by compaction [20, 55, 59], so their influence on reservoir pore space is small at this stage, while the reservoir in ZS is now in the middle diagenetic stage A period as a whole and locally has entered the middle diagenetic stage B period. Carbonate cement with larger crystals is mainly developed, and their occupation of pore space is obvious. The pore space is obviously occupied by carbonate colloids with larger crystals, which seriously destroys the reservoir physical properties.

Laumontite cement is commonly developed in the reservoirs of UUF in ZS, and its content shows a gentle negative correlation with porosity (Figure 15(f)). Zeolite cement is easy to dissolve under acidic conditions and has a certain pore-enhancing effect as the material basis for later dissolution [20, 60], but the content of laumontite in the target reservoir in ZS is very high, resulting in most of the pores being cemented by laumontite and blocking the flow of acidic fluids to a certain extent, so the content of laumontite cement shows a gentle negative correlation with the porosity size.

5.3.3. Effect of Dissolution on Reservoir Physical Properties. The feldspar and lithic fragment content of the reservoir of UUF in ZS is high and contains a certain amount of heterogeneous base. The widespread development of soluble materials such as feldspar, lithic fragment, and matrix provides the material basis for the later dissolution. The reservoir is deeply buried and has experienced strong compaction and cementation, and the whole has entered the period A of middle diagenetic stage, and the local area is already in period B of middle diagenetic stage. The organic matter evolution is in the mature-high maturity stage, producing a large amount of organic acid, which provides an acidic fluid for the dissolution to proceed. Therefore, although UUF has a large burial depth and strong compaction and cementation, a large number of inter- and intragrain pores formed by dissolution are developed in the local depth range, and these pores can improve the reservoir physical properties to a certain extent.

The original pore space of UUF reservoir in ZS has basically disappeared after the complex diagenesis, and the reservoir has poor physical properties, and the porosity shows an obvious decreasing trend with the increase of burial depth (Figure 16). However, there is an obvious secondary pore zone of dissolution genesis in the range of 3750 m-4300 m burial depth. The porosity values of this depth range class of reservoirs are significantly higher than those (theoretical curve values) under normal compaction and cementation conditions, indicating that dissolution has improved the physical properties of the reservoirs and has a positive effect on the formation of high-quality reservoirs.

5.4. Particularity of Glutenite Reservoir. Sedimentation determines the original pore structure of the reservoir, which

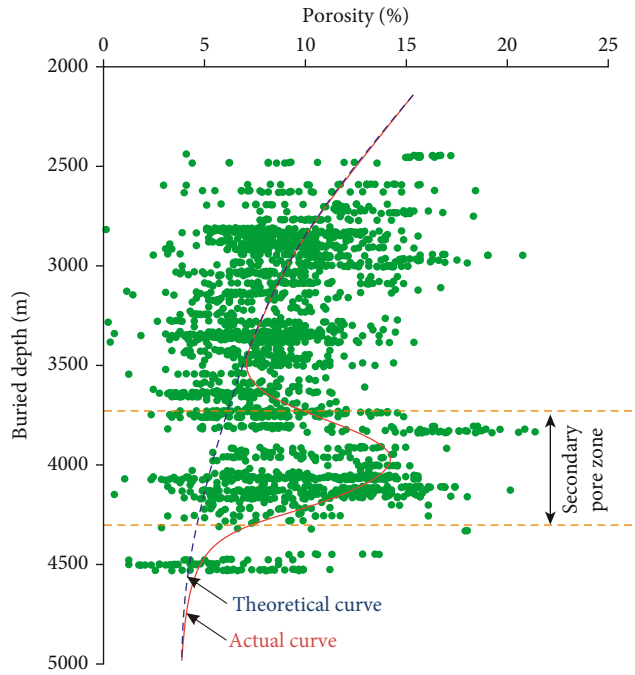

Figure 16: Relationships between porosity with buried depth of UUF in ZS.

is manifested by the different texture and structure of the sediments in different sedimentary facies, especially the facies dominated by glutenite [9, 13, 30, 61]. The sorting of glutenite reservoirs varies greatly and usually poorly sorted. The poorly sorted glutenite has a high content of matrix impurities, which makes it difficult to preserve the intergranular pores, which is shown by the low porosity of the reservoir. Therefore, the porosity of conglomerate is generally smaller than that of sandstone (Figure 9).

However, the permeability of conglomerate is higher than that of sandstone on the whole, which is believed to be the common occurrence of seams distributed along the edges of the gravels in conglomerate reservoirs (Figures 8(a) and 8(b)). They are formed by dewatering and shrinking of mud-filled material during diagenetic, and the majority of them are developed in conglomerates [51, 52]. Previous studies on the pore types of reservoirs of UUF in the Junggar Basin concluded that the seams distributed along the edges of the gravels developed in the reservoir contribute to the physical properties of the reservoir to a certain extent [51, 52, 56, 61].

6. Discussion

(1) The stratigraphy of UUF is mainly conglomerate, followed by sandstone, and the total thickness of mudstone is relatively minimal. The conglomerates and sandstones are mostly gray, gray-green, and gray-brown, and the mudstones are mostly reddish-brown and gray-green

(2) The physical properties of the reservoir of UUF are poor. The permeability of conglomerate is generally larger than that of sandstone. The physical properties

of granule conglomerate and fine pebble conglomerate are relatively better, but the correlation between porosity and permeability is more obvious for coarse pebble conglomerate and fine pebble conglomerate

(3) The reservoirs of UUF in ZS are mainly in the middle diagenetic stage A period. The locally buried deeper areas have entered the middle diagenetic stage B period. The types of diagenesis experienced by the reservoir are mainly compaction, cementation, and dissolution, as well as interstitial material shrinkage and mineral metasomatism

(4) The reservoirs of UUF in ZS have experienced strong compaction and cementation. The physical properties of the reservoir are poor, while the secondary pores formed by dissolution improve the physical properties of the reservoir, which is an important reason why the dense glutenite reservoirs can develop relatively high-quality reservoirs

Data Availability

The data that support the conclusions of this study are available from text and the corresponding author upon reasonable request.

Conflicts of Interest

The authors declare no conflict of interest.

Acknowledgments

We are grateful to the Research Institute of Petroleum Exploration and Development, PetroChina Xinjiang Oilfield, for providing samples and data access. This work was supported by the National Natural Science Foundation of China (Grant number 42130813).

References

[1] Q. C. Li, M. Wu, L. C. Zhao, F. T. Hu, and Z. F. Tang, *The Series of Oil Field Development in China——Development of Conglomerate Oil Field*, Beijing, Petroleum Industry Press, 1997.

[2] Y. Tang, Y. Xu, Y. Z. Li, and L. B. Wang, "Sedimentation model and exploration significance of large-scaled shallow retrogradation fan delta in Mahu sag," *Xinjiang Petroleum Geology*, vol. 39, no. 1, pp. 16–22, 2018.

[3] X. Yu, S. Li, and C. Tan, "Coarse-grained deposits and their reservoir characterizations: a look back to see forward and hot issues," *Journal of Palaeogeography*, vol. 20, no. 5, pp. 713–736, 2018.

[4] D. M. Zhi, Y. Tang, M. L. Zheng, W. J. Guo, T. Wu, and Z. W. Zou, "Discovery, distribution and exploration practice of large oil provinces of above-source conglomerate in Mahu sag," *Xinjiang Petroleum Geology*, vol. 39, no. 1, pp. 1–8, 2018.

[5] Y. Tang, Y. Song, X. G. Guo et al., "Main controlling factors of tight conglomerate oil enrichment above source kitchen in Mahu sag, Junggar Basin," *Acta Petrolei Sinica*, vol. 43, no. 2, pp. 192–206, 2022.

[6] Z. Yang and C. N. Zou, ""Exploring petroleum inside source kitchen": connotation and prospects of source rock oil and gas," *Petroleum Exploration and Development*, vol. 46, no. 1, pp. 181–193, 2019.

[7] Z. Qiu and C. N. Zou, "Unconventional petroleum sedimentology: connotation and prospect," *Acta Sedimentologica Sinica*, vol. 38, no. 1, pp. 1–29, 2020.

[8] X. M. Zhu, R. Pan, S. F. Zhu, W. Wei, and L. Ye, "Research progress and core issues in tight reservoir exploration," *Earth Science Frontiers*, vol. 25, no. 2, pp. 14l–146, 2018.

[9] Q. C. Li, M. Wu, L. C. Zhao et al., "Pore structure comparison and difference mechanism between tight sandstone and tight conglomerate reservoirs," *Acta Geologica Sinica*, vol. 96, no. 6, pp. 2155–2172, 2022.

[10] Y. Tang, W. J. Guo, and X. T. Wang, "New breakthroughs in exploration of conglomerate large oil area in Mahu sag and its enlightenment," *Xinjiang Petroleum Geology*, vol. 40, no. 2, pp. 127–137, 2019.

[11] X. G. Zhou, X. B. Huang, Q. M. Wang, Z. W. Ma, and L. X. Chen, "Identification and description of the multi-stage sandy conglomerate fan body in Shinan steep slope zone, Bohai Sea," *Journal of Northeast Petroleum University*, vol. 44, no. 2, pp. 46–55, 2020.

[12] Q. H. Liu, H. T. Zhu, X. Y. A. Du XF et al., "Development and hotspot of sedimentary response of glutenite in the offshore Bohai Bay basin," *Earth Science*, vol. 45, no. 5, pp. 1676–1705, 2020.

[13] G. F. Zhou and S. T. Gong, "Diagenesis and physical property evolution of tight glutenite reservoir in fault basin: taking Shahezi formation in Xujiaweizi fault depression of Songliao Basin as an example," *Journal of Xi'an Shiyou University (Natural Science Edition)*, vol. 35, no. 1, pp. 34–41, 2020.

[14] Z. H. Zhao, S. J. Xu, X. H. Jiang et al., "Deep strata geologic structure and tight sandy conglomerate gas exploration in Songliao basin, East China," *Petroleum Exploration and Development*, vol. 43, no. 1, pp. 13–25, 2016.

[15] X. Hu, Y. Q. Qu, S. Y. Hu et al., "Geological conditions and exploration potential of shallow oil and gas in slope area of Mahu sag, Junggar Basi," *Lithologic Reservoirs*, vol. 32, no. 2, pp. 67–77, 2020.

[16] J. H. Du, D. M. Zhi, Y. Tang et al., "Prospects in upper Permian and strategic discovery in Shawan sag, Junggar Basin," *China Petroleum Exploration*, vol. 24, no. 1, pp. 24–35, 2019.

[17] W. Z. Zhao, S. Y. Hu, X. J. Guo, J. Z. Li, and Z. L. Cao, "New concepts for deepening hydrocarbon exploration and their application effects in the Junggar Basin, NW China," *Petroleum Exploration and Development*, vol. 46, no. 5, pp. 856–865, 2019.

[18] C. Ding, Y. Q. Pang, Y. L. Meng et al., "Study of the paleoenvironment and reservoir mechanism for volcanic rich clastic reservoirs in the upper Urho formation in the Zhongguai region, Junggar Basin," *Acta Sedimentologica Sinica*, vol. 38, no. 4, pp. 851–867, 2020.

[19] C. M. Zhang, T. J. Yin, Y. Tang et al., "Advances in sedimentological reservoir research in Mahu sag and northwest margin of Junggar Basin," *Journal of Palaeogeography*, vol. 22, no. 1, pp. 129–146, 2020.

[20] Y. P. Ma, X. W. Zhang, L. J. Huang, G. Wang, H. Zhang, and S. Pan, "Characteristics and controlling factors of glutenite reservoir rock quality of retrogradational fan delta: a case study of the upper Wuerhe formation of the Mahu sag, the Junggar

Basin," *Energy Exploration & Exploitation*, vol. 39, no. 6, pp. 2006–2026, 2021.

[21] L. L. Huang, R. Wang, Y. Zou, M. Wang, Q. S. Chang, and Y. X. Qian, "Accumulation characteristics of continuous sand conglomerate reservoirs of upper Permian upper Urho formation in Manan slope area, Junggar Basin," *Petroleum Geology & Experiment*, vol. 44, no. 4, pp. 51–59, 2022.

[22] P. Luo, Y. Qiu, A. Jia, and X. Wang, "The present challenges of Chinese petroleum reservoir geology and research direction," *Acta Sedimentologica Sinica*, vol. 21, no. 1, pp. 142–147, 2003.

[23] Z. Li, J. S. Chen, and P. Guan, "Scientific problems and frontiers of sedimentary diagenesis research in oil-gas-bearing basin," *Acta Petrologica Sinica*, vol. 22, no. 8, pp. 2113–2122, 2006.

[24] J. L. Zhang, P. H. Zhang, and J. Xie, "Diagenesis of clastic reservoirs: advances and prospects," *Advances in Earth Science*, vol. 28, no. 9, pp. 957–967, 2013.

[25] J. L. Luo, C. Li, C. Lei, J. J. Cao, and K. P. Song, "Discussion on research advances and hot issues in diagenesis of clastic-rock reservoirs," *Journal of Palaeogeography*, vol. 22, no. 6, pp. 1021–1040, 2020.

[26] C. D. Curtis, "Possible links between sandstone diagenesis and depth-related geochemical reactions occurring in enclosing mudstones," *Journal of the Geological Society*, vol. 135, no. 1, pp. 107–117, 1978.

[27] R. G. C. Bathurst, *Carbonate Sediments and Their Diagenesis*, Elsevier, Amsterdam, 1971.

[28] V. Schmidt, D. A. McDonald, and R. L. Platt, "Pore geometry and reservoir aspects of secondary porosity in sandstones," *Bulletin of Canadian Petroleum Geology*, vol. 25, no. 2, pp. 271–290, 1977.

[29] S. D. Burley and R. H. Worden, *Sandstone Diagenesis: Recent and Ancient*, Blackwell Publishing, Oxford, 2003.

[30] N. Zhu, Y. C. Cao, K. L. Xi et al., "Diagenesis and physical properties evolution of sandy conglomerate reservoirs: acase study of Triassic Baikouquan formation in northern slope zone of Mahu despression," *Journal of China University of Mining & Technology*, vol. 48, no. 5, pp. 1102–1118, 2019.

[31] L. J. Huang, J. Cao, J. J. Guo, Y. Ma, G. Wang, and H. Zhang, "The forming mechanism of high quality glutenite reservoirs in Baikouquan formation at the eastern slope of Mahu sag of the Junggar basin, China," *Petroleum Science and Technology*, vol. 37, no. 14, pp. 1665–1674, 2019.

[32] H. F. Chen, Q. J. Lv, J. Gao et al., "The characteristics and controlling factors of glutenite reservoirs in the Permian upper Urho Formation, southern Zhongguai Rise, Junggar basin, NW China," *Geological Journal*, vol. 57, no. 1, pp. 221–237, 2022.

[33] J. W. Yu, G. Luo, B. Li et al., "Diagenesis and diagenetic facies of upper Wuerhe formation in the Shawan sag," *Geoscience*, vol. 36, no. 4, pp. 1095–1104, 2022.

[34] F. Wang and Q. C. Ran, "Characteristics of shale reservoir of the first member of Qingshankou formation in northern Songliao Basin," *Lithologic Reservoirs*, vol. 26, no. 5, pp. 64–68, 2014.

[35] L. I. Bo, L. Ü. Yanfang, M. E. Yuanlin et al., "Petrologic characteristics and genetic model of lacustrine lamellar fine- grained rock and its significance for shale oil exploration: a case study of Permian Lucaogou formation in Malang sag, Santanghu basin, NW China," *Petroleum Exploration and Development*, vol. 42, no. 5, pp. 656–666, 2015.

[36] L. I. Bo, S. H. Jiaxin, F. U. Xiaofei et al., "Petrological characteristics and shale oil enrichment of lacustrine fine- grained sedimentary system: a case study of organic-rich shale in first member of Cretaceous Qingshankou formation in Gulong sag, Songliao basin, NE China," *Petroleum Exploration and Development*, vol. 45, no. 5, pp. 884–894, 2018.

[37] X. Wang, J. Hou, S. Li et al., "Insight into the nanoscale pore structure of organic-rich shales in the Bakken formation, USA," *Journal of Petroleum Science and Engineering*, vol. 191, article 107182, 2020.

[38] J. H. Zhao and Z. J. Jin, "Mudstone diagenesis: research advances and prospects," *Acta Sedimentologica Sinica*, vol. 39, no. 1, pp. 58–72, 2021.

[39] L. I. Bo, S. U. Jiahui, Y. Zhang et al., "Reservoir space and enrichment model of shale oil in the first member of Cretaceous Qingshankou formation in the Changling sag, southern Songliao basin, NE China," *Petroleum Exploration and Development*, vol. 48, no. 3, pp. 608–624, 2021.

[40] D. D. Hong, J. Cao, X. G. Guo, B. Bian, and H. Liu, "Diagenetic fluid controls chemical compositions of authigenic chlorite in clastic reservoirs," *Marine and Petroleum Geology*, vol. 137, article 105520, 2022.

[41] C. N. Zou, R. K. Zhu, Z. Q. Chen et al., "Organic-matter-rich shales of China," *Earth-Science Reviews*, vol. 189, pp. 51–78, 2019.

[42] K. H. Yu, Z. J. Zhang, Y. C. Cao et al., "Origin of biogenic-induced cherts from Permian alkaline saline lake deposits in the NW Junggar basin, NW China: implications for hydrocarbon exploration," *Journal of Asian Earth Sciences*, vol. 211, article 104712, 2021.

[43] D. He, C. Yin, and S. Du, "Characteristics of structural segmentation of foreland thrust belts—a case study of the fault belts in the northwestern margin of Junggar basin," *Earth Science Frontiers*, vol. 11, no. 3, pp. 91–101, 2004.

[44] J. Kuang and X. F. Qi, "The structural characteristics and oil-gas explorative direction in Junggar foreland basin," *Xinjiang Petroleum Geology*, vol. 27, no. 1, pp. 5–9, 2006.

[45] X. F. Chen, J. Qi, and H. B. Yang, "Geological characteristics of gas reservoirs in the upper Permian Jiamuhe formation in Zhongguai salient, Junggar basin," *Natural Gas Industry*, vol. 30, no. 9, pp. 19–21, 2010.

[46] X. M. Zhu, *Sedimentary Petrology*, Petroleum Industry Press, Beijing, 2008.

[47] H. Yu, C. Lin, J. Zhou, X. Zhang, and S. Xu, "Reservoir characteristics and influencing factors analysis on early cretaceous Denglouku and Quantou formation in the Yaoyingtai aera of southern Songliao basin," *Acta Sedimentologica Sinica*, vol. 30, no. 2, pp. 240–250, 2012.

[48] H. R. Leroy, *Zeolites and Zeolitic reactions in sedimentary rocks*, Geological Society of America, 1966.

[49] Z. J. Jin, J. Cao, W. X. Hu et al., "Episodic petroleum fluid migration in fault zones of the northwestern Junggar basin (northwest China): evidence from hydrocarbon-bearing zoned calcite cement," *AAPG Bulletin*, vol. 92, no. 9, pp. 1225–1243, 2008.

[50] H. Y. Wu, Y. Tang, and Q. S. Chang, "Genesis of sandy conglomerate reservoirs cemented by zeolites in Jiamuhe formation of Zhongguai swell, Junggar basin," *Xinjiang Petroleum Geology*, vol. 38, no. 3, pp. 281–288, 2017.

[51] S. N. Zhang, X. Q. Ding, Y. L. Wang, D. Xiong, and Z. L. Zhu, "Formation mechanism and distribution of clay minerals of

deeply tight siliciclastic reservoirs," *Journal of Southwest Petroleum University (Science & Technology Edition)*, vol. 34, no. 3, pp. 174–182, 2012.

[52] Y. C. Bao, Q. H. Liu, X. F. Du, W. Wang, and W. L. Shi, "Division of glutenite lithofacies based on the trielement of gravel matrix-fracture," *Earth Science*, vol. 46, no. 6, pp. 2157–2171, 2021.

[53] X. Shan, H. Guo, and Z. Zou, "Diagenesis in alkaline environment and its influences on reservoir quality: a case study of middle-lower Permian clastic reservoirs in northwestern margin of Junggar basin," *Xinjiang Petroleum Geology*, vol. 39, no. 1, pp. 55–62, 2018.

[54] F. X. Ying, D. B. He, Y. M. Long, and X. S. Lin, *Division of Clastic Stage (SY/T 5477-2003)*, Beijing, Petroleum Industry Press, 2003.

[55] J. X. Zhao, D. C. Huang, Y. Luo, Q. Lu, and P. Zhu, "Diagenetic features of reservoirs in the Chang 6 member, south Ordos basin," *Natural Gas Industry*, vol. 29, no. 3, pp. 34–37, 2009.

[56] S. C. Zhang, Z. C. Yang, Z. Y. Liu et al., "Diagenesis constrain to physical property of Permian conglomerate reservoir in underlying bloc of Kebai fault," *Natural Gas Geoscience*, vol. 21, no. 5, pp. 755–761, 2010.

[57] J. F. Tian, Z. L. Chen, and Y. Y. Yang, "Protection mechanism of authigenic chlorite on sandstone reservoir pores," *Geological Science and Technology Information.*, vol. 27, no. 4, pp. 49–54, 2008.

[58] H. Y. Ma, L. F. Zhou, X. G. Zhang, T. Y. Han, J. H. Li, and G. L. Liu, "Diagenesis and favorable diagenetic facies of Chang 8 reservoir in Jiyuan area of Ordos basin," *Petroleum Geology and Experiment*, vol. 35, no. 4, pp. 378–383, 2013.

[59] T. S. Cao, X. F. Tan, L. Luo et al., "Evolution mechanism of differential diagenesis combination and its effect on the reservoir quality in the tight sandstone: a case from the lower Shihezi formation in the Hangjinqi area of Ordos basin, China," *Lithosphere*, vol. 2021, no. Special 1, article 6832767, pp. 1–18, 2021.

[60] J. F. Li, *Formation Mechanism and Reservoir Significance of Diagenetic Zeolites in Permian Glutenite Reservoirs at Zhongguai Area of the Northwestern Junggar Basin, NW China*, Nanjing University, 2019.

[61] B. Chen, X. You, Y. Zhang, S. Zhang, and J. Shi, "Effects of diagenesis and reservoir of the Urho formation in manna region," *Journal of Southwest Petroleum University (Science & Technology Edition)*, vol. 38, no. 1, pp. 10–20, 2016.